ISSN : 0974 - 7486 Volume 13 Issue 4

Materials Science

An Indian Journal

Full Paper

MSAIJ, 13(4), 2015 [136-144]

Corrosion behavior and physical properties of modified tin- antimony bearing alloy

Abu Bakr El- Bediwi, Abbas Al- Bawee*, Mustafa Kamal

Metal Physics Lab., Physics Department, Faculty of Science, Mansoura University, Mansoura, (EGYPT)

Faculty of engineering, University of Diayala, (IRAQ)

ABSTRACT

Effect of adding alloying elements, such as Cu, Bi, Al, Pb, Zn and Ag, on microstructure, corrosion behavior, electrical, thermal and mechanical properties of $SnSb_{13}$ alloy have been investigated. Matrix microstructure, formed phases and other lattice parameters, of $SnSb_{13}$alloy changed after adding alloying elements which effects on all measured physical properties. Corrosion parameters, elastic modulus, internal friction, Vickers hardness, electrical resistivity and thermal parameters of $SnSb_{13}$ alloy varied after adding alloying element. The $Sn_{87}Sb_{10}Bi_3$alloy has lowest corrosion rate but $Sn_{87}Sb_{10}Al_3$ alloy has highest corrosion rate. The $Sn_{87}Sb_{10}Pb_3$alloy has best bearing properties, lower internal friction, self-lubricate and cost, adequate hardness, corrosion resistance, elastic and thermal properties, for automotive applications.

KEYWORDS

White bearing;
Microstructure;
Thermo-elastic properties;
Internal friction;
Corrosion behavior.

INTRODUCTION

Bearing is a device used to transmit loads between relatively moving surfaces or in another word is a device to allow constrained relative motion between two or more parts, typically rotation or linear movement. There is many ways for classifying bearing materials, for example, by the type of material they making up off or by the applications they service. Effects of modification structural on electrical resistivity, elastic modulus, internal friction and hardness of $SnSb_{10}Cu_2X_2$ (X= Pb, Zn, Se, Ag and Cd) has been investigated[1]. The $SnSb_{10}Cu_2Pb_2$ alloy has betters properties for bearing applications. Adding Cu/Pb to Sn-Sb alloy improve their elastic modulus, internal friction, hardness and thermal conductivity[2]. The friction coefficients of WM5, (Sn–20.2%Sb–16.6%Pb–2.6%Cu), are lower than that of WM2, (Sn–7.2%Sb-0.4%Pb-3%Cu), under all scratch test conditions[3]. Structure, hardness, mechanical and electrical transport properties of (90-x) Sn10%SbX%Bi (x = 0, or x e"1) alloys have been studied and analyzed[4]. Effects of solidification rate, microadditions and heating on mechanical properties and micromorphology of Sn- 10.4% Sb alloy have been studied[5, 6]. Creep behaviour, elastic modulus and internal friction of Sn 10%Sb 2%Cu 2%X (X=Pb, Ag, Se, Cd and Zn) alloys have been investigated and stress exponent values have been determined using Mulhearn–Tabor method[6]. The directionally solidified microstructure of Sn-16%Sb hyperperitectic alloy has been investigated at vari-

ous solidification rates using a high-thermal gradient directional solidification apparatus[7]. The aim of this research was to study and analyze the effect of copper, lead, silver, bismuth, aluminum and zinc on corrosion behavior and physical properties of $SnSb_{13}$white bearing.

EXPERIMENTAL WORK

In this work $SnSb_{13-x}X_x$ (X=Bi, Cu, Al, Pb, Zn and Ag & x=3 wt.%) alloys were molten in the muffle furnace using high purity, more than 99.95%, tin, antimony, bismuth, lead, zinc, copper, aluminum and silver. The resulting ingots were turned and re-melted several times to increase the homogeneity of the ingots. From these ingots, long ribbons of about 3-5 mm width and ~ 70 μm thickness were prepared as the test samples by directing a stream of molten alloy onto the outer surface of rapidly revolving copper roller with surface velocity 31 m/s giving a cooling rate of 3.7×10^5 k/s. The samples then cut into convenient shape for the measurements using double knife cuter. Structure of used alloys was performed using an Shimadzu X–ray Diffractometer (Dx–30, Japan)of Cu–Kα radiation with λ=1.54056 Å at 45 kV and 35 mA and Ni–filter in the angular range 2θ ranging from 0 to 100° in continuous mode with a scan speed 5 deg/min. Also Scanning electron microscope JEOL JSM-6510LV, Japan was used to study structure. Electrical resistivity of used alloys was measured by a conventional double bridge method. The melting endotherms of used alloys were obtained using a SDT Q600 V20.9 Build 20 instrument. A digital Vickers micro-hardness tester, (Model-FM-7- Japan), was used to measure Vickers hardness values of used alloys. Internal friction Q^{-1} and the elastic constants of used alloys were determined using the dynamic resonance method[8-10].

RESULTS AND DISCUSSIONS

Structure

X-ray diffraction patternsof $SnSb_{13-x}X_x$ (X=Bi, Cu, Al, Pb, Zn, Ag and x=3 wt. %) rapidly solidified alloys have lines corresponding to β- Sn and SbSn intermetallic phasesas shown in Figure 1. The analysis of x-ray diffraction patterns show that, adding copper, lead, silver, bismuth, aluminum and zinc to $Sn_{87}Sb_{13}$alloy caused a change in matrix microstructure such as lattice parameters and formed crystal structure (crystallinity, crystal size and the orientation). Lattice parameters, (a and c), and unit volume cell of β- Sn phase in $SnSb_{13-x}X_x$alloys were determined and then listed in TABLE (1). Lattice parameters of β- Snin $Sn_{87}Sb_{13}$varied after adding Bi, Cu, Al, Pb, Zn and Ag contents. That is because Bi, Cu, Al, Pb, Zn and Agatoms dissolved in Sn matrix alloy forming a solid solution and other accumulated atoms forming traces of phases.

Scanning electron micrographs, SEM, of $SnSb_{13-x}X_x$ (X=Bi, Cu, Al, Pb, Zn and Ag & x=3 wt. %) alloys show heterogeneity structure, different phases with other soluble atoms, as shown in Figure (2). Microstructure of $SnSb_{13-x}X_x$alloys show β- Sn matrix, SbSnphase and other accumulated atoms forming traces of phasesand that agree with x-ray results.

Thermal properties

Thermal analysis is often used to study solid state transformations as well as solid-liquid reactions. Figure (3) shows DSC thermographs for $SnSb_{13-x}X_x$ (X=Bi, Cu, Al, Pb, Zn,Ag and x=3 wt. %) alloys. Little variation in exothermal peak of $SnSb_{13}$ alloy occurred, which related to a change inSn matrix structure,after adding Bi, Cu, Al, Pb, Zn and Ag contents. The melting temperature and other thermal properties of $SnSb_{13-x}X_x$alloys are listed in TABLE (2). Melting temperature of $SnSb_{13}$alloy decreased after adding Bi, Cu, Al, Pb, Zn and Ag contents.

Elastic modului and internal friction

The elastic constants are directly related to atomic bonding and structure. Elastic modului of $SnSb_{13-x}X_x$alloys are listed in TABLE (3). Elastic modulus of $SnSb_{13}$alloyvaried after adding Bi, Cu, Al, Pb, Zn and Ag contents. The $Sn_{87}Sb_{10}Zn_3$alloy has highest elastic modulus but $Sn_{87}Sb_{10}Al_3$ alloyhas lowest elastic modulus.

The resonance curves $SnSb_{13-x}X_x$alloys are shown in Figure (4). Calculated internal friction and thermal diffusivity of $SnSb_{13-x}X_x$alloys are seen in

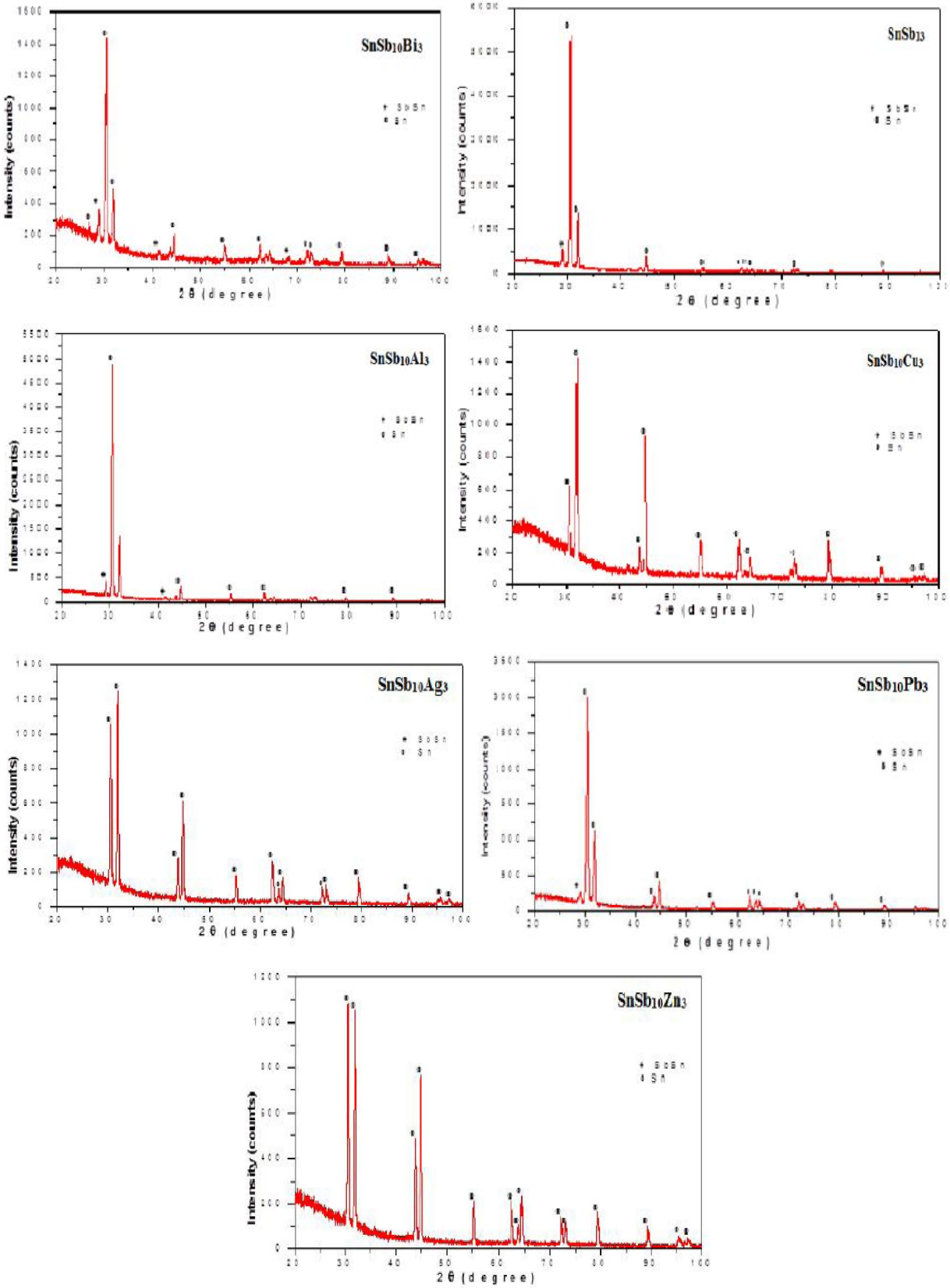

Figure 1 : X-ray diffraction patterns of $SnSb_{13-x}X_x$ alloys

TABLE 1 : Lattice parameters and crystal size of β-Sn in $SnSb_{13-x}X_x$ alloys

Alloys	a Å	c Å	V Å^3	τ Å
$Sn_{87}Sb_{13}$	5.86	3.17	108.735	282.56
$Sn_{87}Sb_{10}Cu_3$	5.85	3.195	109.811	368.89
$Sn_{87}Sb_{10}Bi_3$	5.87	3.176	109.322	329.01
$Sn_{87}Sb_{10}Al_3$	5.86	3.18	109.039	370.45
$Sn_{87}Sb_{10}Pb_3$	5.86	3.174	108.883	355.44
$Sn_{87}Sb_{10}Zn_3$	5.85	3.186	108.898	438.41
$Sn_{87}Sb_{10}Ag_3$	5.85	3.181	109.079	420.09

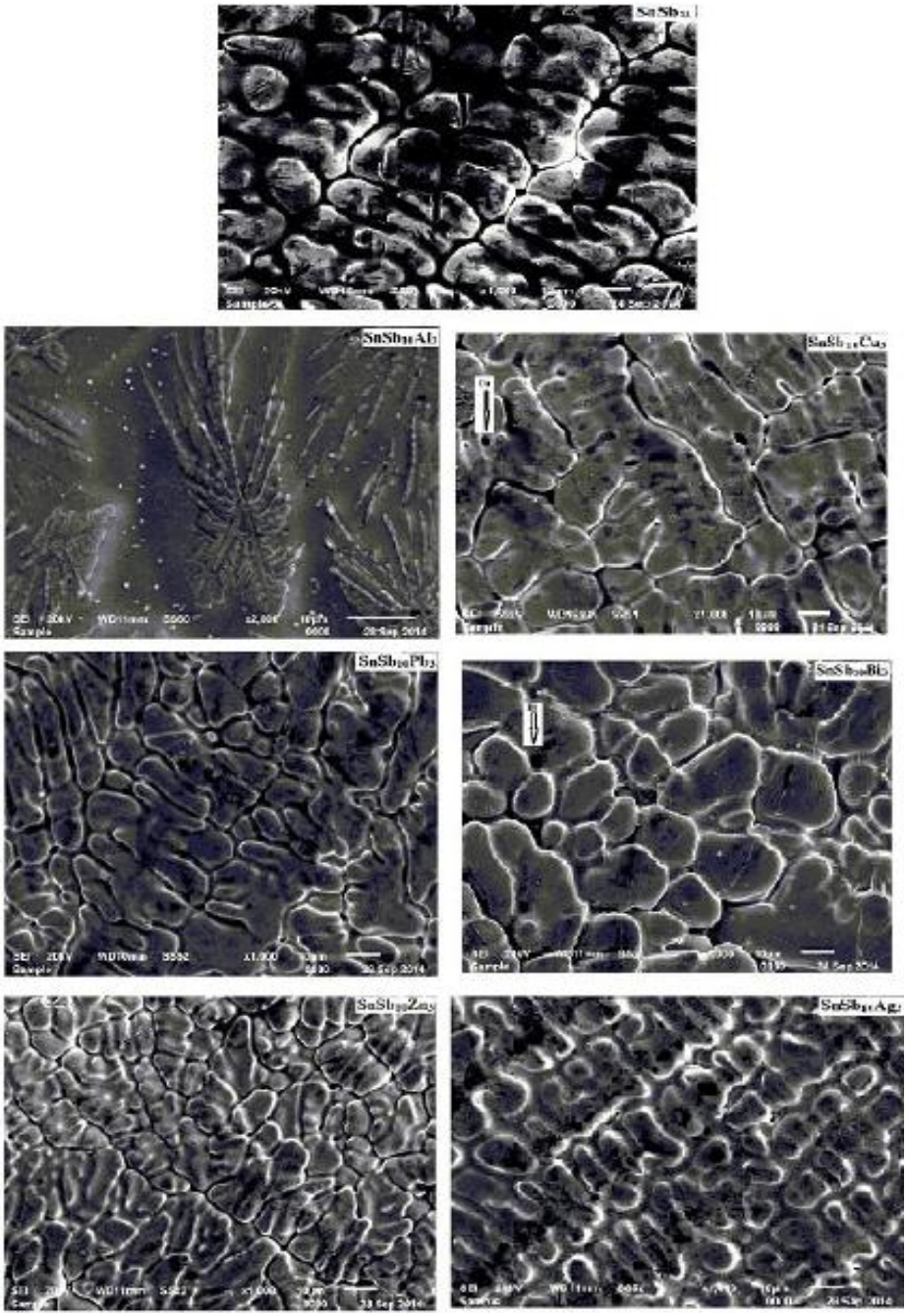

Figure 2 : SEM of $SnSb_{13-x}X_x$ alloys

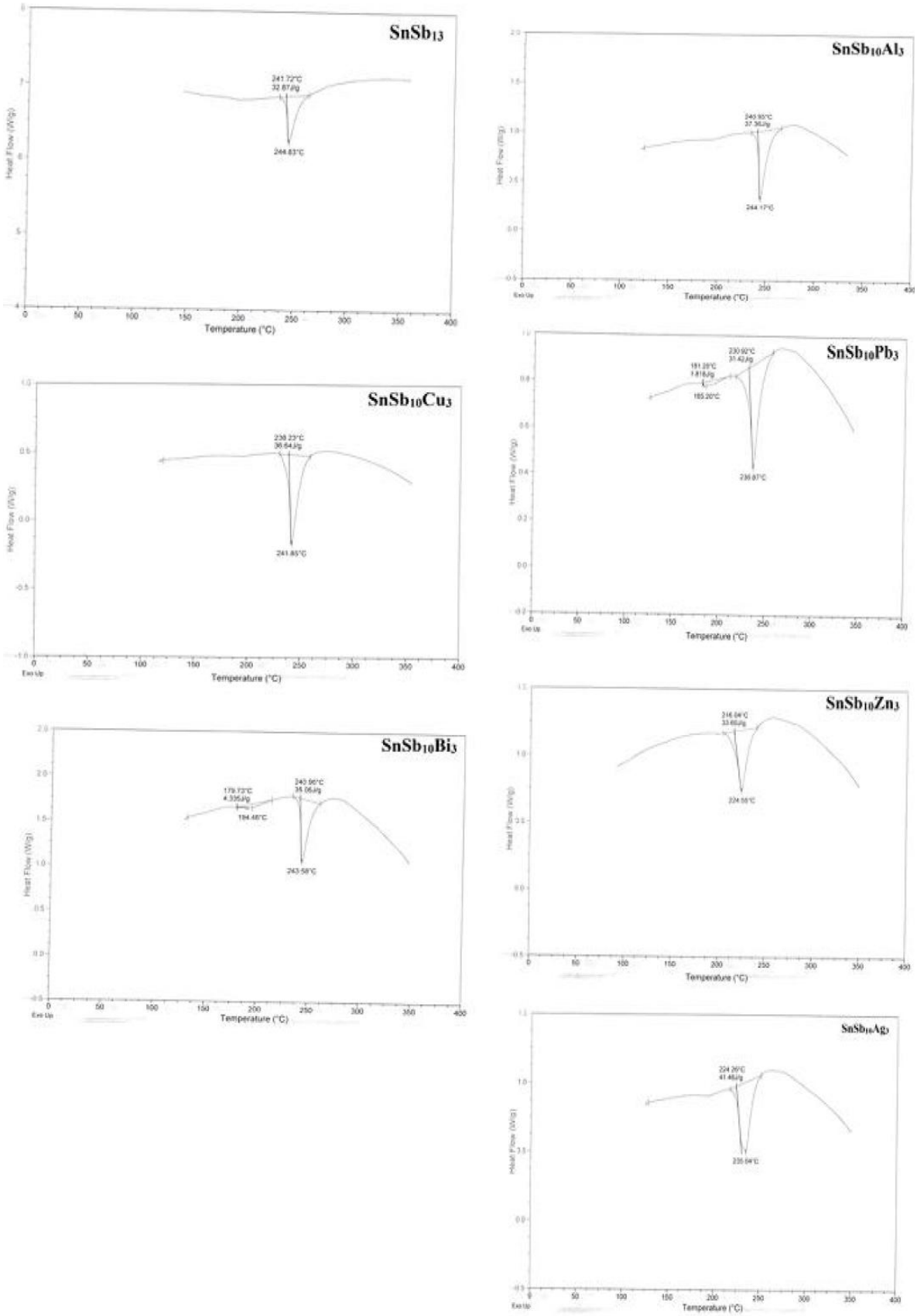

Figure 3 : DSC of $SnSb_{13-x}X_x$ alloys

TABLE 2 : Melting temperature and other thermal properties of $SnSb_{13-x}X_x$alloys

Alloys	Melting point °C	ΔS J/g. °C	C_p J/g. °C
$Sn_{87}Sb_{13}$	244.83	0.132	2.48
$Sn_{87}Sb_{10}Cu_3$	241.85	0.148	1.88
$Sn_{87}Sb_{10}Bi_3$	243.59	0.141	2.45
$Sn_{87}Sb_{10}Al_3$	244.17	0.15	1.12
$Sn_{87}Sb_{10}Pb_3$	236.87	0.131	1.84
$Sn_{87}Sb_{10}Zn_3$	224.55	0.15	1.92
$Sn_{87}Sb_{10}Ag_3$	235.04	0.18	1.65

TABLE 3 : Elastic modului, internal friction and thermal diffusivity of $SnSb_{13-x}X_x$alloys

Alloys	E(GPa)	μ(GPa)	G (GPa)	Q^{-1}	D_{th} x 10^{-8} m^2/sec
$Sn_{87}Sb_{13}$	29.77	10.98	34.48	0.068	12.38
$Sn_{87}Sb_{10}Cu_3$	34.92	12.65	48.58	0.062	8.62
$Sn_{87}Sb_{10}Bi_3$	39.07	14.16	53.90	0.095	2.93
$Sn_{87}Sb_{10}Al_3$	24.24	8.78	34.01	0.091	6.07
$Sn_{87}Sb_{10}Pb_3$	33.02	12.15	39.15	0.025	9.43
$Sn_{87}Sb_{10}Zn_3$	42.11	15.36	54.49	0.05	6.12
$Sn_{87}Sb_{10}Ag_3$	28.23	10.21	40.29	0.037	33.94

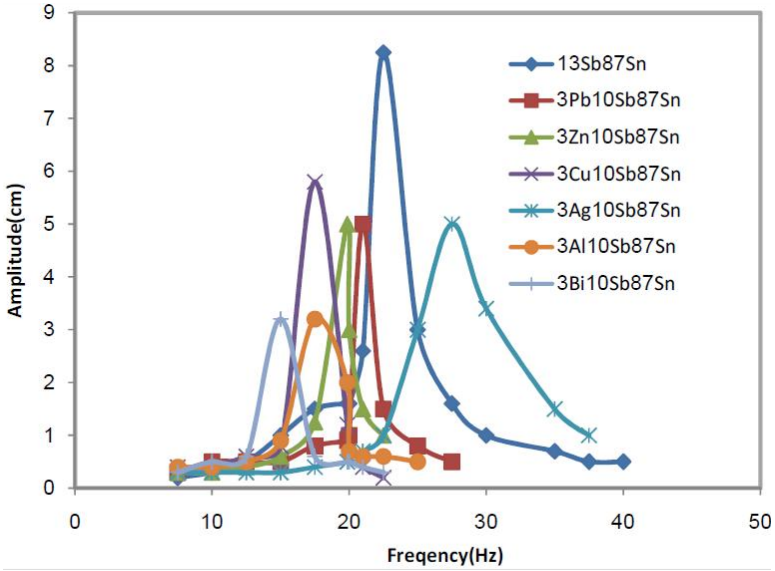

Figure 4 : Resonance curves of $SnSb_{13-x}X_x$ alloys

TABLE 3. Internal friction of $SnSb_{13}$alloyvariedafter adding Bi, Cu, Al, Pb, Zn and Ag contents. The $Sn_{87}Sb_{10}Bi_3$alloy has highest internal friction but $Sn_{87}Sb_{10}Pb_3$ alloy has lowest internal friction.

Vickers microhardness and minimum shear stress

The hardness is the property of material, which gives it the ability to resist being permanently deformed when a load is applied. Vickers hardness of $SnSb_{13-x}X_x$alloys at 10 gram force and indentation time 5 sec are shown in TABLE 4. The minimum shear stress (τ_m) value of $SnSb_{13-x}X_x$alloys was calculated using the equation[9], where $\nu$is Poisson's ratio of the elements in the alloy and then listed in TABLE 4.

$$\tau_m = \frac{1}{2} H_v \left\{ \frac{1}{2}(1-2\nu) + \frac{2}{9}(1+\nu)[2(1+\nu)]^{\frac{1}{2}} \right\}$$

Vickers hardness of $SnSb_{13}$ alloyvariedafter adding Bi, Cu, Al, Pb, Zn and Ag contents. The $Sn_{87}Sb_{10}Cu_3$alloy has lowest hardness but $Sn_{87}Sb_{10}Zn_3$ alloy has highest hardness.

Full Paper

TABLE 4 : Vickers hardness and minimum shear stress ofSnSb13-xXxalloys

Alloys	H_v kg/mm^2	μ_n kg/mm^2
$Sn_{87}Sb_{13}$	23.033±2.1	7.600
$Sn_{87}Sb_{10}Cu_3$	20.42±4.4	6.73
$Sn_{87}Sb_{10}Bi_3$	24.58±5.6	8.11
$Sn_{87}Sb_{10}Al_3$	26.32±4.7	5.38
$Sn_{87}Sb_{10}Pb_3$	28.52±1.8	9.41
$Sn_{87}Sb_{10}Zn_3$	31.78±0.8	14.37
$Sn_{87}Sb_{10}Ag_3$	26.95±4.1	8.89

TABLE 5 : Electrical and thermal conductivities of $SnSb_{13-x}X_x$alloys

Alloys	ρ x10^{-8} Ωm	σ x10^6 $\Omega^{-1}.m^{-1}$	K W.m^{-1}K^{-1}
$Sn_{87}Sb_{13}$	85.95	1.16	1.81
$Sn_{87}Sb_{10}Cu_3$	73.66	1.35	2.1
$Sn_{87}Sb_{10}Bi_3$	59.32	1.68	2.6
$Sn_{87}Sb_{10}Al_3$	73.66	1.35	2.1
$Sn_{87}Sb_{10}Pb_3$	67.3	1.485	2.3
$Sn_{87}Sb_{10}Zn_3$	97.05	1.03	1.61
$Sn_{87}Sb_{10}Ag_3$	91.56	1.09	1.7

TABLE 6 : Corrosion potential, corrosion current and corrosion rate of $SnSb_{13-x}X_x$alloys

Alloys	E_{corr} V	i_{corr} μA cm^{-2}	C.R mpy
$Sn_{87}Sb_{13}$	-0.519	85.00	38.82
$Sn_{87}Sb_{10}Cu_3$	-0.521	144.0	65.81
$Sn_{87}Sb_{10}Bi_3$	-0.764	78.50	35.85
$Sn_{87}Sb_{10}Al_3$	-0.512	154.0	70.19
$Sn_{87}Sb_{10}Pb_3$	-0.519	148.0	67.49
$Sn_{87}Sb_{10}Zn_3$	-0.521	87.90	40.15
$Sn_{87}Sb_{10}Ag_3$	-0.517	98.40	44.95

Electrical resistivity and thermal conductivity

Plastic deformation raises the electrical resistivity as a result of the increased number of electron scattering centers. Crystalline defects serve as scattering center for conduction electrons in metals, so the increase in their number raises the imperfection. Electrical resistivity and calculated electrical and thermal conductivities of $SnSb_{13-x}X_x$alloys are shown in TABLE (5). Electrical resistivity of $SnSb_{13}$ alloyvaried after adding Bi, Cu, Al, Pb, Zn and Ag contents. That is because Bi, Cu, Al, Pb, Zn and Ag atoms dissolved in the alloy matrix playing as scattering center for conduction electronscaused a change in matrix structure of $SnSb_{13}$alloy.

Electrochemical corrosion behavior

Figure (5) shows electrochemical polarization curves for $SnSb_{13-x}X_x$ (X=Bi, Cu, Al, Pb, Zn, Ag and x=3 wt. %) alloysin 0.5 M HCl. From this figure, the corrosion potential of the $SnSb_{13-x}X_x$alloys exhibited a negative potential. Also, the cathodic and the anodic polarization curves showed similar corrosion trends. TABLE (6) presents the corrosion potential (E_{Corr}), corrosion current (I_{Corr}), and corrosion rate ($Corr_{Rate}$) of $SnSb_{13-x}X_x$alloys. The results show that, the corrosion rate in 0.5M HCl of $SnSb_{13}$alloy varied after adding Bi, Cu, Al, Pb, Zn and Ag contents. The $Sn_{87}Sb_{10}Bi_3$alloy has lowest corrosion rate but $Sn_{87}Sb_{10}Al_3$ alloy has highest corrosion rate.That is because adding Bi, Cu, Al, Pb, Zn and Ag contents caused heterogeneous microstructure with affected on microsegregation and reactiv-

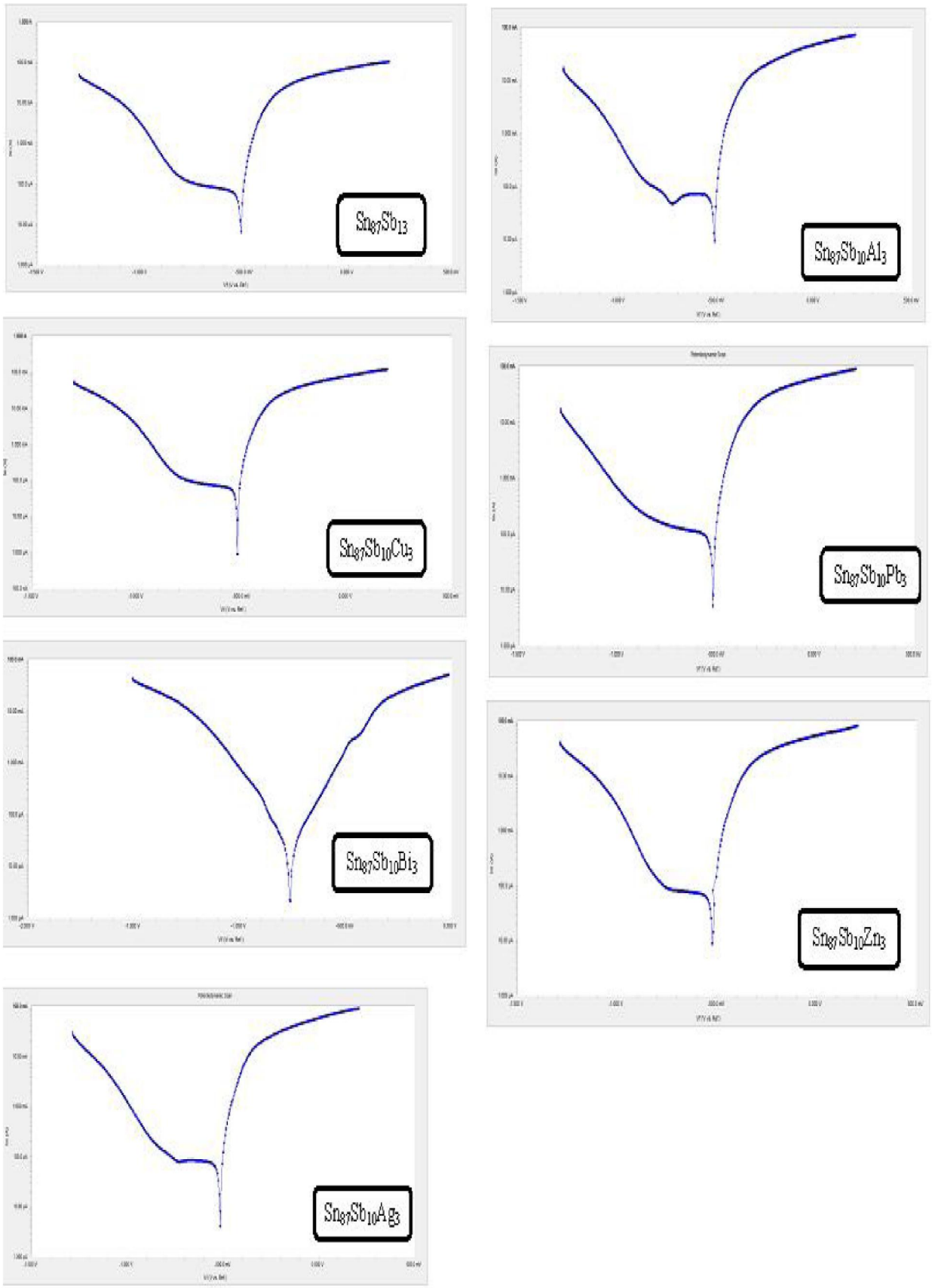

Figure 5 : Electrochemical polarization curves of $SnSb_{13-x}X_x$ alloys

ity of atoms with HCl solution.

CONCLUSIONS

Matrix structure of $SnSb_{13}$ alloy changed after adding Bi, Cu, Al, Pb, Zn and Ag contents due to dissolved atoms forming solid solution and other accumulated atoms forming traces of phases. The $Sn_{87}Sb_{10}Bi_3$alloy has highest internal friction but $Sn_{87}Sb_{10}Pb_3$ alloy has lowest internal friction. The $Sn_{87}Sb_{10}Zn_3$alloy has highest elastic modulus but $Sn_{87}Sb_{10}Al_3$ alloy has lowest elastic modulus. The $Sn_{87}Sb_{10}Cu_3$alloy has lowest hardness but $Sn_{87}Sb_{10}AZn_3$ alloy has highest hardness. The $Sn_{87}Sb_{10}Bi_3$alloy has lowest corrosion rate but $Sn_{87}Sb_{10}Al_3$ alloy has highest corrosion rate.

REFERENCES

[1] A.B.El-Bediwi, A.R.Lashin, A.Mossa, M.Kamal; MSAIJ, **6**, 37 **(2010)**.

[2] M.Kamal, A.El-Bediwi, M.El-Shobaki; Radia.Eff.Def.Sol., **161**, 549 **(2006)**.

[3] M.O.Bora, O.Coban, T.Sinmazcelik, V.Gunay, M.Zeren, Mater.And Design, **31**, 2707 **(2010)**.

[4] A.B.El- Bediwi, El Said Gouda, M.Kamal; AMSE, 65, n° 1, Modeling C- **(2004)**.

[5] M.Kamal, A.Abdel-Salam, J.C.Pieri; J.Mater.Sci., **19**, 3880 **(1984)**.

[6] A.El-Bediwi, A.Lashin, M.Mossa, M.Kamal; Mater.Sci.Engineering A, **528**, 3568 **(2011)**.

[7] H.Xiaowu, L.Shuangming, L.Lin, F.Hengzhi; The Chinese Journal of Nonferrous Metals, **14(1)** 93 **(2004)**.

[8] E.Schreiber, O.L.Anderson, N.Soga; Elastic constant and their measurements, McGraw-Hill, New York, 82 **(1973)**.

[9] S.Timoshenko, J.N.Goddier; "Theory of elasticity, 2nd Edition", McGraw-Hill, New York, 277 **(1951)**.

[10] K.Nuttall; J.Inst.Met., **99**, 266 **(1971)**.